QMEC: A tool for high-throughput quantitative assessment of microbial functional potential in C, N, P, and S biogeochemical cycling

Bang-Xiao Zheng[1,2,3,4], Yong-Guan Zhu[1,5], Jordi Sardans[3,4], Josep Peñuelas[3,4*], Jian-Qiang Su[1**]

[1] *Key Laboratory of Urban Environment and Health, Institute of Urban Environment, Chinese Academy of Sciences, Xiamen 361021, PR China*;
[2] *University of Chinese Academy of Sciences, Beijing 100049, PR China*;
[3] *Consejo Superior de Investigaciones Científicas (CSIC), Global Ecology Unit, Centre for Ecological Research and Forestry Applications (CREAF)–CSIC–Universitat Autonoma de Barcelona (UAB), Bellaterra, 08193 Barcelona, Catalonia, Spain*;
[4] *CREAF, Cerdanyola del Vallès, 08193 Barcelona, Catalonia, Spain*;
[5] *State Key Laboratory of Urban and Regional Ecology, Research Center for Eco-Environmental Sciences, Chinese Academy of Sciences, Beijing 100085, China*.

[*] Corresponding Author
Phone: (+34) 935812199; Fax: (+34) 935814151; E-mail: josep.penuelas@uab.cat

[**] Corresponding Author
Phone: (+86) 592 6190997; Fax: (+86) 592 6190791; E-mail: jqsu@iue.ac.cn

Abstract

Microorganisms are major drivers of elemental cycling in the biosphere. Determining the abundance of microbial functional traits involved in the transformation of nutrients, including carbon (C), nitrogen (N), phosphorus (P) and sulfur (S), is critical for assessing microbial functionality in elemental cycling. We developed a high-throughput quantitative-PCR-based chip, QMEC (Quantitative Microbial Element Cycling), for assessing and quantifying the genetic potential of microbiota to mineralize soil organic matter and to release C, N, P and S. QMEC contains 72 primer pairs targeting 64 microbial functional genes for C, N, P, S and methane metabolism. These primer pairs were characterized by high coverage (average of 18-20 phyla covered per gene) and sufficient specificity (>70% match rate) with a relatively low detection limit (7-102 copies per run). QMEC was successfully applied to soil and sediment samples, identifying significantly different structures, abundances and diversities of the functional genes ($P < 0.05$). QMEC was also able to determine absolute gene abundance. QMEC enabled the simultaneous qualitative and quantitative determination of 72 genes from 72 samples in one run, which is promising for comprehensively investigating microbially mediated ecological processes and biogeochemical cycles in various environmental contexts including those of the current global change.

Key words:

microbial genes, functional potential, high-throughput qPCR, elemental cycling, biogeochemical cycle, ecological process

Introduction

Microorganisms are the major drivers of biogeochemical cycles on Earth (van der Heijden et al., 2008), substantially affecting carbon (C) and sulfur (S) metabolism, organic-matter degradation, nitrogen (N) efflux and phosphorus (P) mobilization in the environment (Zarraonaindia et al., 2013; Vanwonterghem et al., 2014). Those processes may result in CO_2 elevation, greenhouse gases release, nutrient loading and water consumption, which coupled with changes of interacting spheres of the earth (Chapin et al., 2000; Bardgett and van der Putten, 2014). Comprehensive investigation of microbial taxonomic composition and functional-gene diversity and abundance are key for a better understanding of microbially mediated biogeochemical processes and their current global changes (Stevenson and Cole, 1999; Penuelas et al., 2013; Graham et al., 2016).

Culture-independent molecular technologies have been widely adopted to investigate microbial phylogenetic and functional diversity and to evaluate their responses to environmental changes (Zhou et al., 2015; Deng et al., 2016; Feng et al., 2017) . The array-based PhyloChip (a high-density 16S gene oligonucleotide microarray) and high-throughput sequencing of 16S rRNA gene fragments are two commonly reported methods for determining the structure of microbial-community composition (Schmidt et al., 1991; Hazen et al., 2010). Metasequencing, including shotgun metagenomics, metatranscriptomics or their combination, enables the functional characterization of novel genes, phylotypes, regulators and metabolic pathways (Weinstock, 2012). The microarray-based GeoChip is more specific than

sequencing-based technologies for detecting functional genes of interest, especially genes involved in elemental biogeochemistry (Tu et al., 2014).

Sequencing-based metagenomics and hybridization-based microarray technologies have been successfully applied in studies of microbial ecology with high gene coverage and resolution and can generally determine the relative abundance of microbial taxa and functional genes in microbial communities, enabling comparison among environmental samples. Relative abundances are the proportions of specific taxa or genes in microbial communities, enabling the detection of increases or decreases; however, relative abundance cannot well evaluate the impact of microbial-community size on the abundance of taxa and genes. Quantification of absolute abundance, i.e. copy numbers of functional genes or their transcripts, is vital for evaluating the functional capacities and potentials of microbial communities. The prediction of N-cycling processes can be improved more using information of functional-gene abundance than microbial diversity (Graham et al., 2016). Quantitative PCR (qPCR) is the most adopted method to measure the copy number of functional genes. For example, an analysis of oceanic nitrification identified the dominant role of *amo*A (archaeal ammonia mono-oxygenase alpha subunit for aerobic ammonia oxidation) in an archaeal community by correlating its gene abundance with ammonium concentration (Wuchter et al., 2006). The abundances of *amo*A, *nir*K/S and *nos*Z were used to assess the changes in nitrification and denitrification potential across a vegetation gradient (Petersen et al., 2012).

Biogeochemical nutrient cycling is a complex process consisting of numerous steps, each mediated by various functional genes. For example, N cycling is composed of several processes, including N fixation, nitrification, denitrification, ammonification, anaerobic ammonium oxidation, organic N mineralization and assimilatory and dissimilatory N reduction, with over 20 key microbial functional genes involved, including different forms of *nif*H, *amo*A/B, *nap*A, *nar*G, *nir*S/K, *nos*Z, *hzo* and *hzs*A/B (Kuypers et al., 2018). The comprehensive evaluation of microbial functional potential in CNPS biogeochemical cycling requires obtaining quantitative data for all these genes, which is extremely laborious when using conventional qPCR to process many environmental samples. Besides, current knowledge of functional genes involved in P cycling is more limited than for C, N and S cycling. As far as we know, *ppx* (exopolyphosphatase), *ppk* (polyphosphate kinase) and phytase genes are the most reported P-cycling genes (He et al., 2010). Primers for genes responsible for inorganic-P solubilization, alkaline phosphatase (hydrolysis of phosphoric monoesters) and C-P lyase, are not available, which hinders the quantitative evaluation of microbially mediated P cycling. To address these limitations, this study 1) designed a set of primer pairs targeting functional genes involved in P cycling and 2) developed a high-throughput qPCR-based functional-gene chip detection method, QMEC, for the simultaneous quantification of CNPS-cycling genes and further assessment of microbial potentials in CNPS biogeochemical dynamics and microbial responses to environmental changes. QMEC contains 36 reported and 36 novel primer pairs involved in C, N, P and S cycles. The coverage,

specificity and efficiency of the designed primers were validated, and the performance of QMEC was evaluated, by analyzing the functional-gene abundance and diversity of soil and sediment samples.

Results

Specificity and coverage of the designed primers

We designed 36 primer pairs that could potentially amplify genes involved in C, N, P and S cycling (Table S1). These primers annealed to conserved regions of the target genes and produced amplicons averaging 332 bp (ranging from 240 bp for *gdh*A to 464 bp for *xyl*A).

Matched sequences of each gene (434 335 sequences) were phylogenetically analyzed. A total of 42 phyla were represented, with an average of 18 ± 12 phyla and a range of two to 30 phyla per gene. The dominant matched taxa were Alphaproteobacteria (18.4%), Gammaproteobacteria (16.5%) and Actinobacteria (11.4%).

Assessment of QMEC

The HT-qPCR QMEC results were validated by the quantification of the 18 selected genes using conventional real-time qPCR under optimal PCR conditions (Figure 1c). The accuracy for all 18 genes averaged 101.25 ± 8.27%. The abundances of *aps*A, *dsr*B, *hzs*B, *mcr*A, *nir*K1, *nir*S1, *phn*K, *pqq*C and *ure*C quantified by HT-qPCR were very similar (nearly 100% accuracy) to those quantified by conventional qPCR. The average SD and CV of C_T from the replicate samples were 0.22 ± 0.17 and 1.06 ± 0.74%, respectively (Table S2). SD was largest for *gcd* in Q1 at 0.99%, with a CV of

4.90%. Average LOD estimated from the 18 genes (Table S3) was 78.43 ± 27.08 copies per well.

Application of QMEC to environmental samples

QMEC was then applied to the soil and sediment samples to illustrate the patterns of microbial functional-gene structures. Nearly all of the 72 genes were detected; only *hzo* and *hzsA* in soil and *ipu* in sediment were not detected (Table S2). The NMDS analysis identified significantly different functional-gene structures between the soil and sediment, where replicates of each sample clustered together and the soil and sediment samples were well separated along the first axis (Figure 2a). Three replicates of each gene were gathered and many genes were well separated from each other (Figure 2b).

Bacterial populations (16S rRNA gene) and the absolute quantities of the functional genes were significantly larger in all three soil samples than the sediment samples, but the relative abundances of all functional genes were significantly higher in the sediment samples (Figure S1, $P < 0.05$). The clustering analysis of relative gene abundance found that the soils and sediments were well separated into two clusters (Figure 2c, $P < 0.01$). The abundance of functional genes is summarized in Table 1 based on their functions. Nearly all functional genes were significantly more abundant in soil than sediment except for the genes involved in lignin hydrolysis, anaerobic ammonium oxidation and S oxidation (Figure S2, $P < 0.05$), and *mcr*A abundance was also higher in sediment.

The relative abundances of the detected genes were analyzed to determine the differences between the soil and sediment samples. Gene abundance was generally lower in the wheat (H1) than the maize (H2) and soybean (H3) soils, and the abundances of most of the functional genes in H2 and H3 soil differed significantly from those in the sediments ($P < 0.05$). The potentials for starch (*amy*X) and pectin (*pgu*) hydrolysis were significantly higher in H2 than H1 and H3 ($P < 0.05$, Figure 3a), and the abundances of genes for hemicellulose (*abf*A) and cellulose (*cex*) hydrolysis were highest in H3. The abundance of the gene for C fixation (*acc*A) was significantly higher in soil than sediment ($P < 0.05$, Figure 3b). The abundances of *pcc*A, *smt*A, *frd*A, *mct*, *rbc*L and *acs*A were significantly higher in H2 and H3 than H1 ($P < 0.05$). The genes involved in N fixation were 20-fold more abundant in H3 than H1 and H2 (Figure 3c). The *ure*C and *nap*A abundances were significantly higher in soil than sediment, and the genes involved in anaerobic ammonia oxidation (*hzo*, *hzs*A and *hzs*B) were significantly more abundant in sediment ($P < 0.05$). The potentials of organic N mineralization (*gdh*A) and nitrification (*amo*A and *amo*B) were significantly higher in H2 and H3 than H1 ($P < 0.05$). Gene abundance (*bpp*, *cphy*, *pho*D and *pho*X) for organic-P mineralization was significantly higher in soil than sediment, and genes for solubilizing inorganic P (*gcd* and *pqq*C) were significantly more abundant in H2 and H3 than H1 ($P < 0.05$, Figure 3d). The abundances of some genes for S and methane cycling (*dsr*A, *pmo*A and *pqq-mdh*) were highest in H1, but others (*sox*Y, *aps*A and *mxa*F) were significantly higher in H2 and H3 ($P < 0.05$ Figure 3e).

Discussion

Design and assessment of QMEC

This study developed QMEC based on HT-qPCR for comprehensively profiling functional genes involved in C, N, P, S and methane cycling. Many genes are critical to CNPS cycling, but the lack of appropriate primers hinders the quantification of these genes and the further assessment of microbial potential in CNPS cycling. We successfully designed and introduced 36 new primer pairs targeting these genes to supplement the missing genetic tools for analyzing microbially mediated biogeochemical processes. These genes are involved in C hydrolysis, C fixation, methane metabolism and N, P and S cycling. Previous studies of P cycling have focused on a limited set of functional genes, e.g. only three genes were targeted by GeoChip 4.0 (*ppx*, *ppk* and phytase) (Tu et al., 2014), which may be inadequate for the comprehensive evaluation of microbial potentials of organic- or inorganic-P use. We designed and introduced seven new primer pairs to amplify genes involved in P cycling: including two acid phosphatase genes (*bpp*, β-propeller phytase, which is the dominant phytase in water and soil (Lim et al., 2007), and *cphy*, ruminal cysteine phytase (Sebastian and Ammerman, 2009; Ragot et al., 2017)), two alkaline phosphatase genes for phosphate use (*pho*D, which has been identified in 13 bacterial phyla and 71 families in soil (Ragot et al., 2015; Ragot et al., 2017), and *pho*X, which is widely distributed in aquatic systems) and *phn*K, which hydrolyzes organophosphorus compounds (C-P bonds). The organic acid 2-keto-$_{D}$-gluconic acid

has a high ability to solubilize inorganic P (Hwangbo et al., 2003), which requires a pyrroloquinoline quinone (PQQ) co-factor. We thus designed primer pairs for a PQQ-dependent glucose dehydrogenase gene (*gcd*) and its cofactor gene *pqq*C for assessing the potential for inorganic-P solubilization.

Primer pairs targeting genes with the same function but covering extended taxa were also designed and introduced in QMEC. Conventional *nir*K and *nir*S primers (*nir*K1 and *nir*S1 in this study) typically cover denitrifiers from Alpha-, Beta- and Gammaproteobacteria (Katsuyama et al., 2008; Yoshida et al., 2012). The recently reported *nir*K and *nir*S primers (*nir*K2, *nir*K3, *nir*S2 and *nir*S3 in this study) with a greater diversity of targets, including Actinobacteria, Bacteroidetes, Chloroflexi and Euryarchaeota, were also introduced for comprehensively estimating denitrifying potential (Wei et al., 2015).

The specificity and phylogenetic coverage of the primers designed in this study were assessed by BLAST searches against the NCBI database and the analysis of amplicon sequences. These primers covered an average of 18 ± 5 phyla. All newly designed primers had >70% specificity, and 20 primers had >80% specificity (Figure 1a), suggesting that the designed primers were applicable in functional-gene detection. The 20-30% mismatch rate may have been due to the unified HT-qPCR protocol to ensure the simultaneous detection of multiple functional genes rather than to suboptimal amplifying conditions of primer pairs. The phylogenetic analysis identified distinct taxonomic compositions of functional genes between the soil- and

sediment-derived sequences, (Figure 1b), suggesting that the coverage of the designed primers was sufficient to identify various taxa under different environment contexts.

Annealing temperature is critical for accurate amplification since diverse annealing temperatures may alter primer-binding kinetics and result in quantification bias, especially in using primers with degenerate positions (Lueders and Friedrich, 2003; Gaby and Buckley, 2017). One benefit of HT-qPCR based on SmartChip Reat-time PCR system was one-time amplifying of numerous genes with one PCR protocol, which has been extensively proved to be efficient in antibiotic resistance gene amplification (Chen et al., 2016; Zhu et al., 2017). For further confirm, the accuracy and precision of QMEC were tested by comparing the results for 18 randomly selected genes to those using conventional qPCR. The amplification accuracies of QMEC were similar to those for conventional qPCR (Figure 1c, nearly 100%), suggesting that the QMEC protocol could simultaneously detect multiple genes. The CV was low (1.06 ± 0.74%, Table S2), indicating that QMEC amplification was stable and precise. This finding was in accordance with a previous report that WaferGen SmartChip were capable of C_T standard deviations <0.2 or CVs <3% (Saunders, 2013).

Application of QMEC

QMEC was further applied for profiling functional genes in soils and estuary sediments. Functional-gene structure, gene abundance and gene diversity (Figures 2c, 3, S3 & S4) differed significantly between soil and sediment. Interestingly, the

relative and absolute abundances of most of the functional genes were reversed between the soil and sediment samples (Figure 2c). For example, the absolute abundance of *acs*A was highest in H2, but its relative abundance was highest in Q3. Absolute gene abundance in pooled replicate samples from one site were well separated from the abundance in samples from different sites (Figure 2a), and absolute gene abundance differed significantly ($P < 0.05$) between soil and sediment and between different soils (Figure 3), suggesting that QMEC could successfully differentiate between functional-gene profiles of different environments. QMEC can quantify absolute gene abundance (copy number), unlike metagenomic sequencing and microarrays (Figure S2). Gene copy number of functional gene reflects the absolute quantities of functional genes in one environmental sample based on qPCR technology. This technology is commonly applied in ecological studies and believed to be precise, high-sensitive, reproducible and easy-to-interpret. Previous studies have found that key biochemical processes were strongly associated with absolute functional-gene copy numbers. For example, the absolute abundances of various N-cycling genes, including *nif*H, *amo*A, *nir*S, *nir*K and *nos*Z, were sensitive to long-term N enrichment in a steppe ecosystem (Zhang et al., 2013). The absolute abundances of *nir*S, *nir*K and other N functional genes were able to account for differences in denitrifying rate, ammonia availability and rate of nitrate transformation in different wastewater-treatment systems (Wang et al., 2015; Wang et al., 2016). Although currently GeoChip and metagenomics are used to acquire microbial functional genes and their structures and to relate them to biogeochemical processes,

the gene copy number obtained by qPCR is still of vital importance. For example, GeoChip was applied in a deep-sea hydrothermal vent to determine the differences of metabolic function between samples; however, the qPCR method was also used to quantify the gene copy number of 16S rRNA, mcrA, cbbL and cbbM gene, interpreting the abundance difference between bacterial and archaea community, uncovering the potentials of predominant biogeochemical process (methane metabolism and CO2 fixation) and making relations with functional community (Wang et al., 2009). A report in Antarctic area used GeoChip to detect the variation of functional genes with different chemical and biogeochemical properties; however, the most highly detected N- and C-cycles genes were also precisely quantified by qPCR to evaluate the functional redundancy (ammonia oxidation, C-fixation, methane oxidation and generation, etc.) among the dominant microbial community members (Yergeau et al., 2007). Similar examples could be found in previous studies (Zhou et al., 2008; Trivedi et al., 2012).

The RNA-level measurements could provide information about microbial community dynamics because the RNA could directly relate to the specific function of protein synthesis (Blazewicz et al., 2013). Elser, *et al*. also indicated the RNA, especially ribosomal RNA (rRNA) as rapid protein synthesis, directly or indirectly related with evolutionary processes and consequently ecological dynamics (Elser et al., 2000). However, the RNA abundance may not always be a greater biogeochemical indicator than DNA. For instance, a survey of planktonic *Crenarchaea* in the Pacific Ocean indicated that the gene abundance (copy number) of *amoA*, which expressed

ammonia monooxygenase subunit A for aerobic oxidation of ammonia, strongly correlated with ocean depth while the transcript of *amoA* gene (RNA level) showed non-significant relevance (Church et al., 2010). The meta-transcriptome analysis or high-throughput sequencing of RNA genes may comprehensively give a functional profiles of gene expression. For example, a pyrosequencing analysis of microbial community RNA in ocean surface waters, which produces large amounts of cDNA fragments, proved that the genes of key metabolic pathway could be obtained and the abundance of key genes favorably compared to independent qPCR assessments of individual gene expression (Frias-Lopez et al., 2008). However, the pyrosequencing-based technology, no matter in DNA or RNA level, is prone to artifacts where single DNA fragments are duplicately sequenced, which limited its application to relate with biogeochemical potentials. As Gifford, *et al*. have indicated that qPCR approaches can provide absolute numbers with greater sensitivity, the actual limitation is simultaneous detection of a handful of functional genes (Gifford et al., 2011).

The idea of QMEC provides an effective solution to both accurate quantification and simultaneous detection. However, as all the degenerate primer designer may face, there existed a non-target amplification of our designed and cited primers. The best way to avoid this problem is to massively expand testing samples and their types, which is far more than easy to achieve in this study. The best usage of QMEC is to make choices of really needed primers rather than using all of them.

Materials and Methods

QMEC is a qPCR-based chip containing 71 microbial CNPS primers and 1 bacterial taxa primer, which could parallel quantify 72 DNA samples or 24 samples with 3 replicates in one time.

QMEC primers

QMEC contained a total of 72 primer pairs: 36 designed pairs, 35 published pairs and one pair targeting the bacterial 16S rRNA gene as the reference gene (Table S1). Most published primer pairs originated from previous studies, including those targeting a new functional gene (*pqq*C) from a recent study (Zheng et al., 2017) or genes with extended phylogenies such as *nir*K2, *nir*K3, *nir*S2 and *nir*S3. We designed 36 novel primer pairs, in which primers specific for *acs*A, *kor*A, *lig*, *mmo*X, *phn*K, *pqq-mdh*, *ppx*, *sox*Y and *yed*Z genes were designed based on the conserved regions of amino acid sequences aligned using ClustalW2 (Larkin et al., 2007). Degenerate primers for *abf*A, *acc*A, *acs*E, *amy*A, *amy*X, *apu*, *cda*R, *cdh*, *cex*, *chi*A, *exo-chi*, *frd*A, *gcd*, *gdh*A, *glx*, *ipu*, *man*B, *mct*, *mnp*, *naglu*, *pccA*, *pgu*, *pox*, *ppk*, *sga*, *smt*A and *xyl*A were designed using Primer Premier 5.0 (Lalitha, 2000).

Soil and sediment sampling

Samples of surface soils (0-15 cm) from wheat (*Triticum aestivum* L.) (H1), maize (*Zea mays* L.) (H2) and soybean (*Glycine max* L.) (H3) fields were collected after harvest in June 2014 from a long-term cropped site in Hailun, Heilongjiang, China

(47°26'N, 126°38'E). The samples were lyophilized, sieved (2.0 mm) and stored at -20 °C for further analysis. Sediment samples (top 15 cm) (Q1, Q2 and Q3) were collected using a grab sampler from the estuary of the Qiantang River in Hangzhou, Zhejiang, China (30°39'N, 120°52'E) during summer 2013 (Figure S3) (Zhu et al., 2017). All samples were transferred to the laboratory on dry ice and stored at -20 °C before analysis.

DNA extraction and quantification

DNA was extracted from the soil and sediment samples using the FastDNA Spin Kit for Soil (MP Biomedicals, Santa Ana, USA) following the manufacturer's instructions. DNA quality was checked by ultraviolet absorbance (ND1000, NanoDrop, Thermo Fisher Scientific, Waltham, USA). DNA concentration was determined using the QuantiFluor dsDNA kit (Promega, Fitchburg, USA). DNA extracts were diluted to 50 ng μL^{-1} with sterilized water and stored at -20 °C before use.

Validation of primers

The specificity and taxonomic coverage of the 36 designed primer pairs were assessed by sequence analysis of the corresponding amplicons from the environmental samples. The DNA extracts from the soil (H1-H3) and sediment (Q1-Q3) samples were equally mixed as soil- and sediment-derived DNA templates (HD and QD, respectively). Each 50-μL PCR reaction contained 25 μL of *Premix Ex Taq* (TAKARA, Dalian, China), 0.2 μM each primer, 1 ng μL^{-1} DNA template and 0.1 mg

340 mL^{-1} bovine serum albumin. The samples were amplified with an initial denaturation
341 at 95 °C for 5 min and 35 cycles of denaturation at 95 °C for 30 s, annealing at 58 °C
342 for 30 s and extension at 72 °C for30 s, followed by a final extension at 72 °C for 5
343 min. The PCR products were purified (Universal DNA purification kit, TIANGEN,
344 Beijing, China), quantified (QuantiFluor dsDNA kit, Promega), pooled at equal molar
345 concentrations and sequenced using an Illumina Hiseq2500 platform (Novogen,
346 Tianjin, China). The raw reads were filtered and aligned with bacterial sequences in
347 the Reference Sequence (RefSeq) database (ftp://ftp.ncbi.nlm.nih.gov/refseq/release)
348 using Local Blast 2.2.27+ (ftp://ftp.ncbi.nlm.nih.gov/blast/executables/blast+/2.2.27/).
349 The e-value of the alignments was set at 10^{-5}, and the highest score was accepted. The
350 aligned result with hypothetical protein was excluded. All sequences were submitted
351 to the National Center for Biotechnology Information Sequence Read Archive with
352 the accession numbers SRP107153 and SRP107154.

353 *HT-qPCR*

354 The H1-H3 soil and Q1-Q3 sediment samples were used as examples for QMEC
355 detection quantified by HT-qPCR (SmartChip Real-time PCR system, WaferGen
356 Biosystems, Fremont, USA) using the 16S rRNA gene (F525/R907) as the reference
357 gene (Su et al., 2015). The chip reaction systems were prepared following manual
358 instructions. The qPCR protocol was an initial denaturation at 95 °C for 10 min with
359 40 cycles of denaturation at 95 °C for 30 s, annealing at 58 °C for 30 s and extension
360 at 72 °C for 30 s. The melting curve was automatically generated by the WaferGen

software. Three replicates of each sample were amplified to analyze the reproducibility of QMEC. Results with multiple melting peaks or amplification efficiencies <80% and >120% were excluded by the SmartChip qPCR software. The results with a threshold cycle (C_T) <31 were used for further analysis. Relative copy number was calculated as described by (Looft et al., 2012). Relative gene abundance was defined as the proportion of the abundance of a functional gene to the abundance of the 16S rRNA gene (equation 1). Absolute gene abundance was calculated based on the absolute 16S rRNA gene copy number quantified by conventional qPCR where *Fun* and *16S* indicate the functional and 16S rRNA genes, respectively (equation 2) (Zhu et al., 2017).

Gene relative copy number $GR = (31 - C_T)/\left({}^{10}/_{3}\right)$ (1)

Gene absolute copy number $GA_{Fun} = \frac{GA_{16S} \cdot GR_{Fun}}{GR_{16S}}$ (2)

Assessment of QMEC

We randomly selected 18 genes (the 16S rRNA gene, *aps*A, *cda*R, *chi*A, *dsr*B, *frd*A, *hzs*B, *man*B, *mcr*A, *nif*H, *nir*K1, *nir*S1, *phn*K, *pho*D, *pqq*C, *rbc*L, *smt*A and *ure*C) for quantification by conventional real-time qPCR (LightCycler 480, Hoffmann-La Roche, Basel, Switzerland) for comparison with the results from the HT-qPCR. The 16S rRNA gene was used as the reference gene (Zheng et al., 2017). DNA from the HD and QD samples was prepared (n=3) and used for quantification in the LightCycler 480 System. The reaction mixture consisted of 0.2 μM each primer, 10 ng

of template DNA and 1× SYBR premix Ex *Taq*. The protocols for the various genes are listed in Table S4. Standard plasmids of each genes were prepared by amplifying the 18 genes in 50-μL volumes containing 1 μL of *Premix Ex Taq* (TAKARA), 0.2 μM each primer and 1 ng μL^{-1} DNA template. The amplicons were then inserted into pMD 19-T vectors (TAKARA). The concentration of plasmid DNA was measured using a QuantiFluor dsDNA kit (Promega). qPCR Standard curves were generated using 10-fold serially diluted plasmid DNA with 90-110% amplification efficiency. The copy numbers of the target genes were calculated based on the standard curve and were compared with those generated from the QMEC results.

The limit of detection (LOD) of QMEC was determined using 10-fold serial dilutions of the standard plasmids of the 18 genes from 10^6 to 10^{12} copies μL^{-1}, with at least three replicates for quantification. The reaction system and protocol were the same as for the HT-qPCR described above. Replicates with C_T standard deviations <1 were included in the calculation of LOD.

Statistical Analysis

Mean, standard deviation (SD) and coefficient of variation (CV, the ratio of SD to mean) were calculated using Office 365. Correlation and variance (ANOVA) analyses used SPSS Statistics 21.0. Bar plotting and cluster figure generation, nonmetric multidimensional scaling (NMDS), an analysis of similarity (ANOSIM) and a heatmap analysis were conducted using the ggplot2 (Ito and Murphy, 2013), plotly

401 (Sievert et al., 2016), vegan (Oksanen et al., 2013) and pheatmap (Kolde and Kolde,

402 2015) packages of RStudio version 3.4.2, respectively.

403

Compliance and ethics

None declared.

Acknowledgements

This work was financially supported by the Strategic Priority Research Program of the Chinese Academy of Sciences (XDB15020402, XDB15020302) and the Natural Science Foundation of China (41571130063, 41430858). J. P. and J. S. acknowledge the financial support from the European Research Council Synergy grant ERC-SyG-2013-610028 IMBALANCE-P.

Figure Legends

Figure 1. Assessment of QMEC. (a) Specificity of the 36 designed primer pairs. The specificities are based on alignment with the Reference Sequence (RefSeq) database. (b) Relative abundances of the dominant bacterial phyla in the soil and sediment samples using the 36 pairs. (c) Accuracy of QMEC for the 18 randomly selected genes. The accuracy indicates the ratio of HT-qPCR copy number to conventional qPCR copy number. Relative abundances are based on the proportions of DNA sequences classified at the phylum level.

Figure 2. Nonmetric multidimensional scaling (NMDS) analyses of (a) all replicates of the six soil and sediment samples and (b) functional genes with three replicates based on their abundance and diversity. (c) Heatmap analysis of absolute functional-gene abundances (left) and relative abundances (right). The plotted values were natural-logarithm transformed.

Figure 3. Analysis of functional-gene differences between soil and sediment. Three soils with different plant hosts (H1-H3) were compared to sediment samples (Q). (a) Differences in abundance of C-hydrolysis genes. The genes are arranged by the biodegradability of their target substrates, from labile to recalcitrant. Differences in the abundances of genes involved in (b) C fixation, (c) N processes and (d) P cycling. (e) Differences in the abundances of genes involved in methane metabolism and S cycling. Error bars represent standard errors. Different letters indicate

433 significant differences between soil samples at $P < 0.05$. ** indicates significant

434 differences between soil and sediment samples at $P < 0.05$.

References

Baker, M., 2011. qPCR: quicker and easier but don't be sloppy. Nat Methods 8, 207-212.

Bardgett, R.D., van der Putten, W.H., 2014. Belowground biodiversity and ecosystem functioning. Nature 515, 505-511.

Blazewicz, S.J., Barnard, R.L., Daly, R.A., Firestone, M.K., 2013. Evaluating rRNA as an indicator of microbial activity in environmental communities: limitations and uses. ISME J 7, 2061-2068.

Chapin, F.S., 3rd, Zavaleta, E.S., Eviner, V.T., Naylor, R.L., Vitousek, P.M., Reynolds, H.L., Hooper, D.U., Lavorel, S., Sala, O.E., Hobbie, S.E., Mack, M.C., Diaz, S., 2000. Consequences of changing biodiversity. Nature 405, 234-242.

Chen, Q.L., An, X.L., Li, H., Su, J.Q., Ma, Y., Zhu, Y.G., 2016. Long-term field application of sewage sludge increases the abundance of antibiotic resistance genes in soil. Environ Int 92-93, 1-10.

Chen, Y., Gelfond, J.A., McManus, L.M., Shireman, P.K., 2009. Reproducibility of quantitative RT-PCR array in miRNA expression profiling and comparison with microarray analysis. BMC Genomics 10, 407.

Church, M.J., Wai, B., Karl, D.M., DeLong, E.F., 2010. Abundances of crenarchaeal *amo*A genes and transcripts in the Pacific Ocean. Environ Microbiol 12, 679-688.

455 De Wilde, B., Lefever, S., Dong, W., Dunne, J., Husain, S., Derveaux, S., Hellemans,
456 J., Vandesompele, J., 2014. Target enrichment using parallel nanoliter
457 quantitative PCR amplification. BMC Genomics 15.
458 Deng, Y., He, Z.L., Xiong, J.B., Yu, H., Xu, M.Y., Hobbie, S.E., Reich, P.B., Schadt,
459 C.W., Kent, A., Pendall, E., Wallenstein, M., Zhou, J.Z., 2016. Elevated carbon
460 dioxide accelerates the spatial turnover of soil microbial communities. Glob
461 Chang Biol 22, 957-964.
462 Elser, J.J., Sterner, R.W., Gorokhova, E., Fagan, W.F., Markow, T.A., Cotner, J.B.,
463 Harrison, J.F., Hobbie, S.E., Odell, G.M., Weider, L.J., 2000. Biological
464 stoichiometry from genes to ecosystems. Ecol Lett 3, 540-550.
465 Feng, W., Liang, J., Hale, L.E., Jung, C.G., Chen, J., Zhou, J., Xu, M., Yuan, M., Wu,
466 L., Bracho, R., Pegoraro, E., Schuur, E.A.G., Luo, Y., 2017. Enhanced
467 decomposition of stable soil organic carbon and microbial catabolic potentials by
468 long-term field warming. Glob Chang Biol 23, 4765-4776.
469 Frias-Lopez, J., Shi, Y., Tyson, G.W., Coleman, M.L., Schuster, S.C., Chisholm, S.W.,
470 DeLong, E.F., 2008. Microbial community gene expression in ocean surface
471 waters. Proc Nat Acad Sci USA 105, 3805-3810.
472 Gaby, J.C., Buckley, D.H., 2017. The use of degenerate primers in qPCR analysis of
473 functional genes can cause dramatic quantification bias as revealed by
474 investigation of *nif*H primer performance. Microb Ecol 74, 701-708.

475 Gifford, S.M., Sharma, S., Rinta-Kanto, J.M., Moran, M.A., 2011. Quantitative
476 analysis of a deeply sequenced marine microbial metatranscriptome. ISME J 5,
477 461-472.
478 Graham, E.B., Knelman, J.E., Schindlbacher, A., Siciliano, S., Breulmann, M.,
479 Yannarell, A., Beman, J., Abell, G., Philippot, L., Prosser, J., 2016. Microbes as
480 engines of ecosystem function: when does community structure enhance
481 predictions of ecosystem processes? Front Microbiol 7.
482 Hazen, T.C., Dubinsky, E.A., DeSantis, T.Z., Andersen, G.L., Piceno, Y.M., Singh, N.,
483 Jansson, J.K., Probst, A., Borglin, S.E., Fortney, J.L., Stringfellow, W.T., Bill,
484 M., Conrad, M.E., Tom, L.M., Chavarria, K.L., Alusi, T.R., Lamendella, R.,
485 Joyner, D.C., Spier, C., Baelum, J., Auer, M., Zemla, M.L., Chakraborty, R.,
486 Sonnenthal, E.L., D'Haeseleer, P., Holman, H.Y., Osman, S., Lu, Z., Van
487 Nostrand, J.D., Deng, Y., Zhou, J., Mason, O.U., 2010. Deep-sea oil plume
488 enriches indigenous oil-degrading bacteria. Science 330, 204-208.
489 He, Z., Deng, Y., Van Nostrand, J.D., Tu, Q., Xu, M., Hemme, C.L., Li, X., Wu, L.,
490 Gentry, T.J., Yin, Y., Liebich, J., Hazen, T.C., Zhou, J., 2010. GeoChip 3.0 as a
491 high-throughput tool for analyzing microbial community composition, structure
492 and functional activity. ISME J 4, 1167-1179.
493 He, Z., Deng, Y., Zhou, J., 2012. Development of functional gene microarrays for
494 microbial community analysis. Curr Opin Biotech 23, 49-55.

Hwangbo, H., Park, R.D., Kim, Y.W., Rim, Y.S., Park, K.H., Kim, T.H., Suh, J.S., Kim, K.Y., 2003. 2-Ketogluconic acid production and phosphate solubilization by Enterobacter intermedium. Curr Microbiol 47, 0087-0092.

Ito, K., Murphy, D., 2013. Application of ggplot2 to Pharmacometric Graphics. CPT Pharmacometrics Syst Pharmacol 2, e79.

Katsuyama, C., Kondo, N., Suwa, Y., Yamagishi, T., Itoh, M., Ohte, N., Kimura, H., Nagaosa, K., Kato, K., 2008. Denitrification activity and relevant bacteria revealed by nitrite reductase gene fragments in soil of temperate mixed forest. Microb Environ 23, 337-345.

Kolde, R., Kolde, M.R., 2015. Package 'pheatmap'.

Kuypers, M.M.M., Marchant, H.K., Kartal, B., 2018. The microbial nitrogen-cycling network. Nat Rev Microbiol 16, 263-276.

Lalitha, S., 2000. Primer premier 5. Biotech Software & Internet Report: The Computer Software Journal for Scient 1, 270-272.

Langille, M.G., Zaneveld, J., Caporaso, J.G., McDonald, D., Knights, D., Reyes, J.A., Clemente, J.C., Burkepile, D.E., Vega Thurber, R.L., Knight, R., Beiko, R.G., Huttenhower, C., 2013. Predictive functional profiling of microbial communities using 16S rRNA marker gene sequences. Nat Biotechnol 31, 814-821.

Larkin, M.A., Blackshields, G., Brown, N.P., Chenna, R., McGettigan, P.A., McWilliam, H., Valentin, F., Wallace, I.M., Wilm, A., Lopez, R., Thompson, J.D., Gibson, T.J., Higgins, D.G., 2007. Clustal W and clustal X version 2.0. Bioinformatics 23, 2947-2948.

517 Liang, Y., Van Nostrand, J.D., Deng, Y., He, Z., Wu, L., Zhang, X., Li, G., Zhou, J.,
518 2011. Functional gene diversity of soil microbial communities from five oil-
519 contaminated fields in China. ISME J 5, 403-413.
520 Lim, B.L., Yeung, P., Cheng, C., Hill, J.E., 2007. Distribution and diversity of
521 phytate-mineralizing bacteria. ISME J 1, 321-330.
522 Looft, T., Johnson, T.A., Allen, H.K., Bayles, D.O., Alt, D.P., Stedtfeld, R.D., Sul,
523 W.J., Stedtfeld, T.M., Chai, B., Cole, J.R., Hashsham, S.A., Tiedje, J.M., Stanton,
524 T.B., 2012. In-feed antibiotic effects on the swine intestinal microbiome. Proc
525 Natl Acad Sci USA 109, 1691-1696.
526 Lu, Z., Deng, Y., Van Nostrand, J.D., He, Z., Voordeckers, J., Zhou, A., Lee, Y.J.,
527 Mason, O.U., Dubinsky, E.A., Chavarria, K.L., Tom, L.M., Fortney, J.L.,
528 Lamendella, R., Jansson, J.K., D'Haeseleer, P., Hazen, T.C., Zhou, J., 2012.
529 Microbial gene functions enriched in the Deepwater Horizon deep-sea oil plume.
530 ISME J 6, 451-460.
531 Lueders, T., Friedrich, M.W., 2003. Evaluation of PCR amplification bias by terminal
532 restriction fragment length polymorphism analysis of small-subunit rRNA and
533 mcrA genes by using defined template mixtures of methanogenic pure cultures
534 and soil DNA extracts. Appl Environ Microbiol 69, 320-326.
535 Mamanova, L., Coffey, A.J., Scott, C.E., Kozarewa, I., Turner, E.H., Kumar, A.,
536 Howard, E., Shendure, J., Turner, D.J., 2010. Target-enrichment strategies for
537 next-generation sequencing. Nat Methods 7, 111-118.

538 Oksanen, J., Blanchet, F.G., Kindt, R., Legendre, P., Minchin, P.R., O'hara, R.,
539 Simpson, G.L., Solymos, P., Stevens, M.H.H., Wagner, H., 2013. Package
540 'vegan'. Community ecology package, version 2.
541 Penuelas, J., Poulter, B., Sardans, J., Ciais, P., van der Velde, M., Bopp, L., Boucher,
542 O., Godderis, Y., Hinsinger, P., Llusia, J., Nardin, E., Vicca, S., Obersteiner, M.,
543 Janssens, I.A., 2013. Human-induced nitrogen-phosphorus imbalances alter
544 natural and managed ecosystems across the globe. Nat Commun 4.
545 Petersen, D.G., Blazewicz, S.J., Firestone, M., Herman, D.J., Turetsky, M., Waldrop,
546 M., 2012. Abundance of microbial genes associated with nitrogen cycling as
547 indices of biogeochemical process rates across a vegetation gradient in Alaska.
548 Environ Microbiol 14, 993-1008.
549 Ragot, S.A., Kertesz, M.A., Bunemann, E.K., 2015. *pho*D alkaline phosphatase gene
550 diversity in soil. Appl Environ Microbiol 81, 7281-7289.
551 Ragot, S.A., Kertesz, M.A., Meszaros, E., Frossard, E., Bunemann, E.K., 2017. Soil
552 phoD and phoX alkaline phosphatase gene diversity responds to multiple
553 environmental factors. FEMS Microbiol Ecol 93.
554 Saunders, N.A., 2013. Real-time PCR Arrays. Real-time PCR: Advanced
555 Technologies and Applications, 199.
556 Schmidt, T.M., DeLong, E.F., Pace, N.R., 1991. Analysis of a marine picoplankton
557 community by 16S rRNA gene cloning and sequencing. J Bacteriol 173, 4371-
558 4378.

559 Sebastian, M., Ammerman, J.W., 2009. The alkaline phosphatase PhoX is more
560 widely distributed in marine bacteria than the classical PhoA. ISME J 3, 563.
561 Sievert, C., Parmer, C., Hocking, T., Chamberlain, S., Ram, K., Corvellec, M.,
562 Despouy, P., 2016. plotly: Create interactive web graphics via Plotly's JavaScript
563 graphing library [Software].
564 Stevenson, F.J., Cole, M.A., 1999. Cycles of soils: carbon, nitrogen, phosphorus,
565 sulfur, micronutrients. John Wiley & Sons.
566 Su, J.Q., Wei, B., Ou-Yang, W.Y., Huang, F.Y., Zhao, Y., Xu, H.J., Zhu, Y.G., 2015.
567 Antibiotic resistome and its association with bacterial communities during
568 sewage sludge composting. Environ Sci Technol 49, 7356-7363.
569 Trivedi, P., He, Z., Van Nostrand, J.D., Albrigo, G., Zhou, J., Wang, N., 2012.
570 Huanglongbing alters the structure and functional diversity of microbial
571 communities associated with citrus rhizosphere. ISME J 6, 363-383.
572 Tu, Q., Yu, H., He, Z., Deng, Y., Wu, L., Van Nostrand, J.D., Zhou, A., Voordeckers,
573 J., Lee, Y.J., Qin, Y., Hemme, C.L., Shi, Z., Xue, K., Yuan, T., Wang, A., Zhou,
574 J., 2014. GeoChip 4: a functional gene-array-based high-throughput
575 environmental technology for microbial community analysis. Mol Ecol Resour
576 14, 914-928.
577 van der Heijden, M.G.A., Bardgett, R.D., van Straalen, N.M., 2008. The unseen
578 majority: soil microbes as drivers of plant diversity and productivity in terrestrial
579 ecosystems. Ecol Lett 11, 296-310.

580 Vanwonterghem, I., Jensen, P.D., Ho, D.P., Batstone, D.J., Tyson, G.W., 2014.
581 Linking microbial community structure, interactions and function in anaerobic
582 digesters using new molecular techniques. Curr Opin Biotechnol 27, 55-64.
583 Wang, F., Zhou, H., Meng, J., Peng, X., Jiang, L., Sun, P., Zhang, C., Van Nostrand,
584 J.D., Deng, Y., He, Z., Wu, L., Zhou, J., Xiao, X., 2009. GeoChip-based analysis
585 of metabolic diversity of microbial communities at the Juan de Fuca Ridge
586 hydrothermal vent. Proc Natl Acad Sci USA 106, 4840-4845.
587 Wang, H., Ji, G., Bai, X., He, C., 2015. Assessing nitrogen transformation processes
588 in a trickling filter under hydraulic loading rate constraints using nitrogen
589 functional gene abundances. Bioresource Technol 177, 217-223.
590 Wang, L., Zhang, Y., Luo, X., Zhang, J., Zheng, Z., 2016. Effects of earthworms and
591 substrate on diversity and abundance of denitrifying genes (*nir*S and *nir*K) and
592 denitrifying rate during rural domestic wastewater treatment. Bioresource
593 Technol 212, 174-181.
594 Wei, W., Isobe, K., Nishizawa, T., Zhu, L., Shiratori, Y., Ohte, N., Koba, K., Otsuka,
595 S., Senoo, K., 2015. Higher diversity and abundance of denitrifying
596 microorganisms in environments than considered previously. ISME J 9, 1954-
597 1965.
598 Weinstock, G.M., 2012. Genomic approaches to studying the human microbiota.
599 Nature 489, 250-256.
600 Wuchter, C., Abbas, B., Coolen, M.J., Herfort, L., van Bleijswijk, J., Timmers, P.,
601 Strous, M., Teira, E., Herndl, G.J., Middelburg, J.J., Schouten, S., Sinninghe

602 Damste, J.S., 2006. Archaeal nitrification in the ocean. Proc Natl Acad Sci USA
603 103, 12317-12322.
604 Yergeau, E., Kang, S., He, Z., Zhou, J., Kowalchuk, G.A., 2007. Functional
605 microarray analysis of nitrogen and carbon cycling genes across an Antarctic
606 latitudinal transect. ISME J 1, 163-179.
607 Yoshida, M., Ishii, S., Fujii, D., Otsuka, S., Senoo, K., 2012. Identification of active
608 denitrifiers in rice paddy soil by DNA-and RNA-based analyses. Microb Environ
609 27, 456-461.
610 Zarraonaindia, I., Smith, D.P., Gilbert, J.A., 2013. Beyond the genome: community-
611 level analysis of the microbial world. Biol & Philos 28, 261-282.
612 Zhang, X., Liu, W., Schloter, M., Zhang, G., Chen, Q., Huang, J., Li, L., Elser, J.J.,
613 Han, X., 2013. Response of the abundance of key soil microbial nitrogen-cycling
614 genes to multi-factorial global changes. PLoS One 8, e76500.
615 Zheng, B.X., Hao, X.L., Ding, K., Zhou, G.W., Chen, Q.L., Zhang, J.B., Zhu, Y.G.,
616 2017. Long-term nitrogen fertilization decreased the abundance of inorganic
617 phosphate solubilizing bacteria in an alkaline soil. Sci Rep-UK 7.
618 Zhou, J., He, Z., Yang, Y., Deng, Y., Tringe, S.G., Alvarez-Cohen, L., 2015. High-
619 throughput metagenomic technologies for complex microbial community
620 analysis: open and closed formats. MBio 6.
621 Zhou, J., Kang, S., Schadt, C.W., Garten, C.T., Jr., 2008. Spatial scaling of functional
622 gene diversity across various microbial taxa. Proc Natl Acad Sci USA 105, 7768-
623 7773.

624 Zhu, Y.G., Zhao, Y., Li, B., Huang, C.L., Zhang, S.Y., Yu, S., Chen, Y.S., Zhang, T.,
625 Gillings, M.R., Su, J.Q., 2017. Continental-scale pollution of estuaries with
626 antibiotic resistance genes. Nat Microbiol 2.

Supporting Information

Table S1. QMEC primer pairs.

Table S2. Mean, standard deviation (SD) and coefficient of variation (CV) of cycle threshold (CT number) for each gene in the soil and sediment samples.

Table S3. Limit of detection (LoD) for the 18 randomly selected genes.

Table S4. Amplification protocols for the 18 randomly selected genes for real-time qPCR.

Figure S1. Abundance and relative ratio of 16S rDNA and total functional genes in the soil and sediment samples.

Figure S2. Abundance of functional genes in the soil and sediment samples.

Figure S3. Sediment sampling sites in Qiantang Estuary, Hangzhou Bay.

Table 1. Summary of functional-gene abundance.

Gene category	Gene number	Gene names	Gene abundance (copies × 10^7 g^{-1} soil)					
			H1	H2	H3	Q1	Q2	Q3
C cycling	**35**							
Carbon hydrolysis	18							
Starch	5	*amy*A, *amy*X, *apu*, *sga*, *ipu*	43.93 ± 15.15 bc	135.3 ± 38.43 a	13.01 ± 4.573 d	20.13 ± 1.388 cd	31.01 ± 3.056 cd	64.03 ± 9.818 b
Hemicellulose	3	*abf*A, *man*B, *xyl*A	27.01 ± 3.920 cd	88.37 ± 10.64 a	71.09 ± 10.30 b	9.228 ± 0.465 e	14.34 ± 0.696 de	31.87 ± 2.906 c
Cellulose	3	*cdh*, *cex*, *naglu*	7.147 ± 1.278 cd	21.03 ± 5.546 a	15.73 ± 2.155 b	3.218 ± 0.144 d	4.897 ± 0.413 d	9.239 ± 1.507 c
Chitin	2	*chi*A, *exo-chi*	3.319 ± 1.629 bc	8.546 ± 1.532 a	7.251 ± 1.937 a	1.852 ± 0.216 c	2.497 ± 1.132 c	4.752 ± 0.676 b
Pectin	1	*pgu*	1.640 ± 0.236 cd	5.341 ± 0.356 b	7.023 ± 0.852 a	0.408 ± 0.102 e	1.032 ± 0.183 de	2.279 ± 0.289 c
Lignin	4	*glx*, *lig*, *mnp*, *pox*	26.50 ± 12.49 b	77.38 ± 13.47 a	17.33 ± 3.776 bc	11.67 ± 1.571 c	24.43 ± 1.941 bc	71.69 ± 8.096 a
C fixation	13	*acc*A, *acl*B, *acs*A, *acs*B, *acs*E, *frd*A, *cda*R, *kor*A, *mcr*A, *mct*, *pcc*A, *rbc*L, *smt*A	282.3 ± 76.16 c	757.6 ± 136.5 a	769.8 ± 115.4 a	132.5 ± 7.144 d	224.0 ± 18.81 cd	464.5 ± 62.61 b
Methane metabolism	4							
Methane production	2	*mxa*F, *pqq-mdh*	14.64 ± 5.961 d	43.15 ± 5.451 b	71.21 ± 15.72 a	11.01 ± 1.067 e	14.94 ± 1.445 d	22.52 ± 0.564 c
Methane oxidation	2	*mmo*X, *pmo*A	7.704 ± 2.294 c	25.66 ± 6.044 a	27.59 ± 6.419 a	6.135 ± 0.358 c	9.343 ± 0.661 c	16.02 ± 2.108 b
N cycling	**22**							
N fixation	1	*nif*H	0.791 ± 0.297 b	2.623 ± 0.292 b	31.70 ± 4.262 a	1.394 ± 0.046 b	1.360 ± 0.093 b	1.022 ± 0.252 b
Nitrification	4	*amo*A1, *amo*A2, *amo*B, *hao*, *nxr*A	23.53 ± 9.141 d	105.7 ± 16.26 a	66.05 ± 10.75 b	13.70 ± 3.023 d	26.14 ± 2.589 cd	40.76 ± 4.386 c
Denitrification	9	*nar*G, *nir*K1, *nir*K2, *nir*K3, *nir*S1, *nir*S2, *nir*S3, *nos*Z1, *nos*Z2	97.36 ± 23.98 bc	304.7 ± 55.08 a	357.2 ± 73.10 a	60.71 ± 10.04 c	104.0 ± 8.829 bc	126.9 ± 17.32 b
Ammonification	1	*ure*C	34.53 ± 8.571 b	86.40 ± 21.53 a	81.10 ± 10.91 a	3.718 ± 0.284 c	5.058 ± 0.236 c	7.049 ± 1.215 c
Anaerobic ammonium oxidation	3	*hzo*, *hzs*A, *hzs*B	0.039 ± 0.027 b	0.087 ± 0.009 b	0.093 ± 0.013 b	0.080 ± 0.022 b	0.139 ± 0.015 b	0.786 ± 0.177 a
Assimilatory N reduction	1	*nas*A	0.035 ± 0.007 c	0.267 ± 0.048 b	0.793 ± 0.106 a	0.032 ± 0.004 c	0.091 ± 0.029 c	0.108 ± 0.018 c
Dissimilatory N reduction	1	*nap*A	1.857 ± 0.397 c	5.317 ± 0.716 a	2.748 ± 0.370 b	0.547 ± 0.069 d	0.637 ± 0.079 d	0.671 ± 0.079 d
Organic N mineralization	1	*gdh*A	14.31 ± 3.632 bc	44.77 ± 6.415 a	52.52 ± 11.62 a	8.270 ± 2.268 c	14.12 ± 2.306 bc	21.98 ± 1.712 b
P cycling	**9**							
Organic P mineralization	5	*bpp*, *cphy*, *phn*K, *pho*D, *pho*X	67.47 ± 29.84 bc	181.9 ± 35.04 a	120.1 ± 33.62 b	20.04 ± 1.751 c	33.51 ± 2.430 c	79.20 ± 60.76 bc
Inorganic P solubilization	3	*gcd*, *pqq*C	17.87 ± 3.411 b	70.94 ± 20.22 a	46.66 ± 37.61 ab	3.891 ± 0.332 e	6.484 ± 0.285 d	8.810 ± 1.108 c
Inorganic P biosynthesis	1	*ppk*	0.185 ± 0.085 c	0.471 ± 0.119 b	0.782 ± 0.105 a	0.178 ± 0.029 c	0.297 ± 0.063 c	0.489 ± 0.086 b
Inorganic P hydrolysis	1	*ppx*	104.4 ± 52.52 cd	286.9 ± 38.77 b	359.4 ± 60.22 a	67.81 ± 11.96 d	93.15 ± 13.82 cd	153.8 ± 23.04 c
S cycling	**5**							
S reduction	3	*aps*A, *dsr*A, *dsr*B	23.75 ± 8.191 d	80.17 ± 12.81 b	109.2 ± 16.01 a	17.28 ± 1.275 d	24.97 ± 4.329 d	43.06 ± 5.872 c
S oxidation	2	*sox*Y, *yed*Z	16.39 ± 2.048 c	54.00 ± 11.53 a	46.83 ± 16.40 a	16.73 ± 3.162 c	27.87 ± 2.802 bc	39.77 ± 8.108 ab
Phylogenetic marker	**1**	16S rRNA gene	312.7 ± 68.49 b	519.2 ± 66.00 a	576.8 ± 77.56 a	60.66 ± 3.062 c	71.81 ± 3.857 c	86.20 ± 12.14 c

Means ± standard errors. Different letters within a row indicate significant differences at $P < 0.05$.

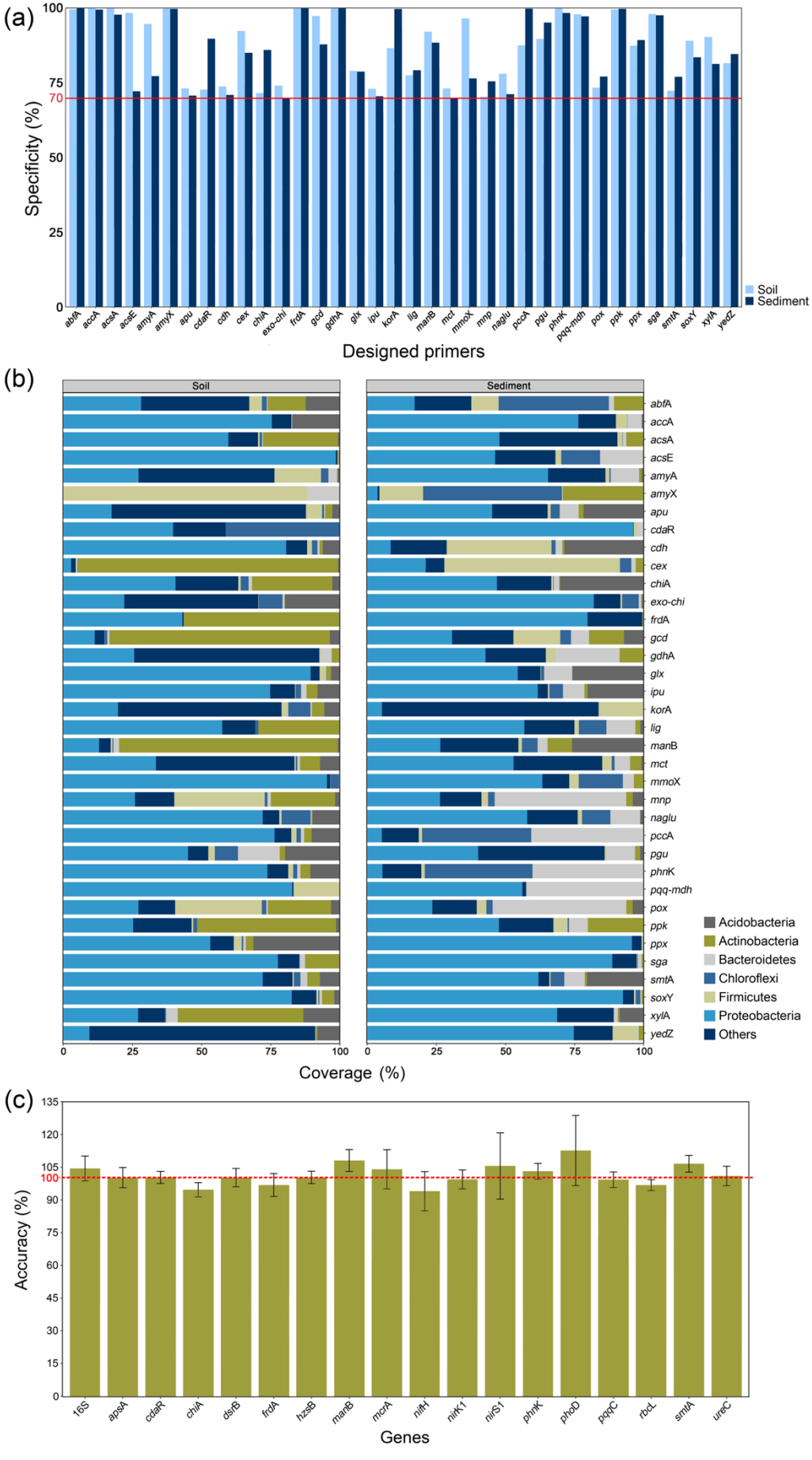

643

644 **Figure 1**

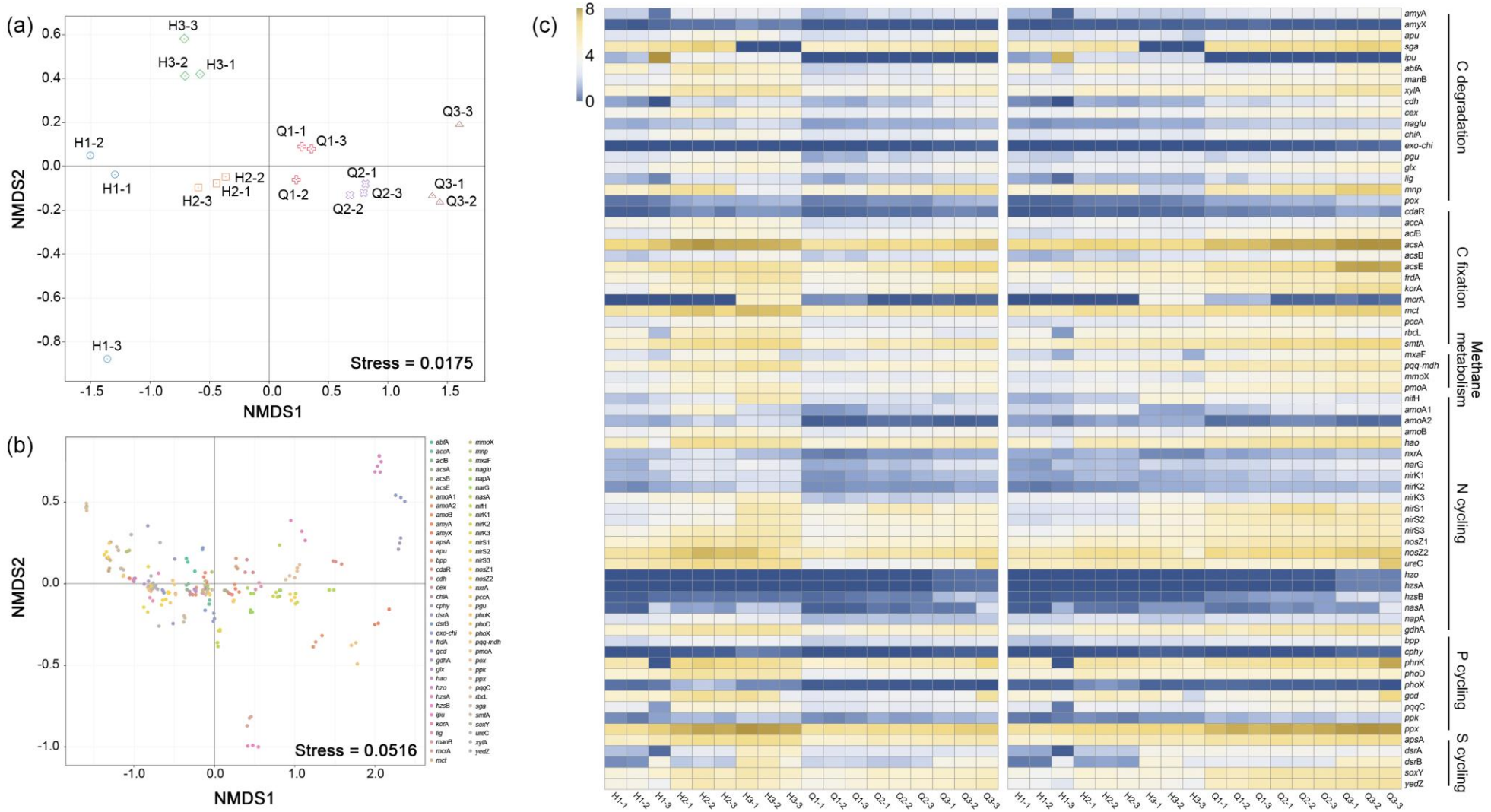
(a)
H3-3
H3-2
H3-1
Q3-3
Q1-1
Q1-3
H1-2
Q2-1
H2-2
Q3-1
H1-1
H2-1
Q1-2
Q2-3
H2-3
Q2-2
Q3-2
H1-3
Stress = 0.0175
NMDS1
NMDS2
(b)
Stress = 0.0516
NMDS1
NMDS2
(c)
C degradation
C fixation
Methane metabolism
N cycling
P cycling
S cycling

Figure 2

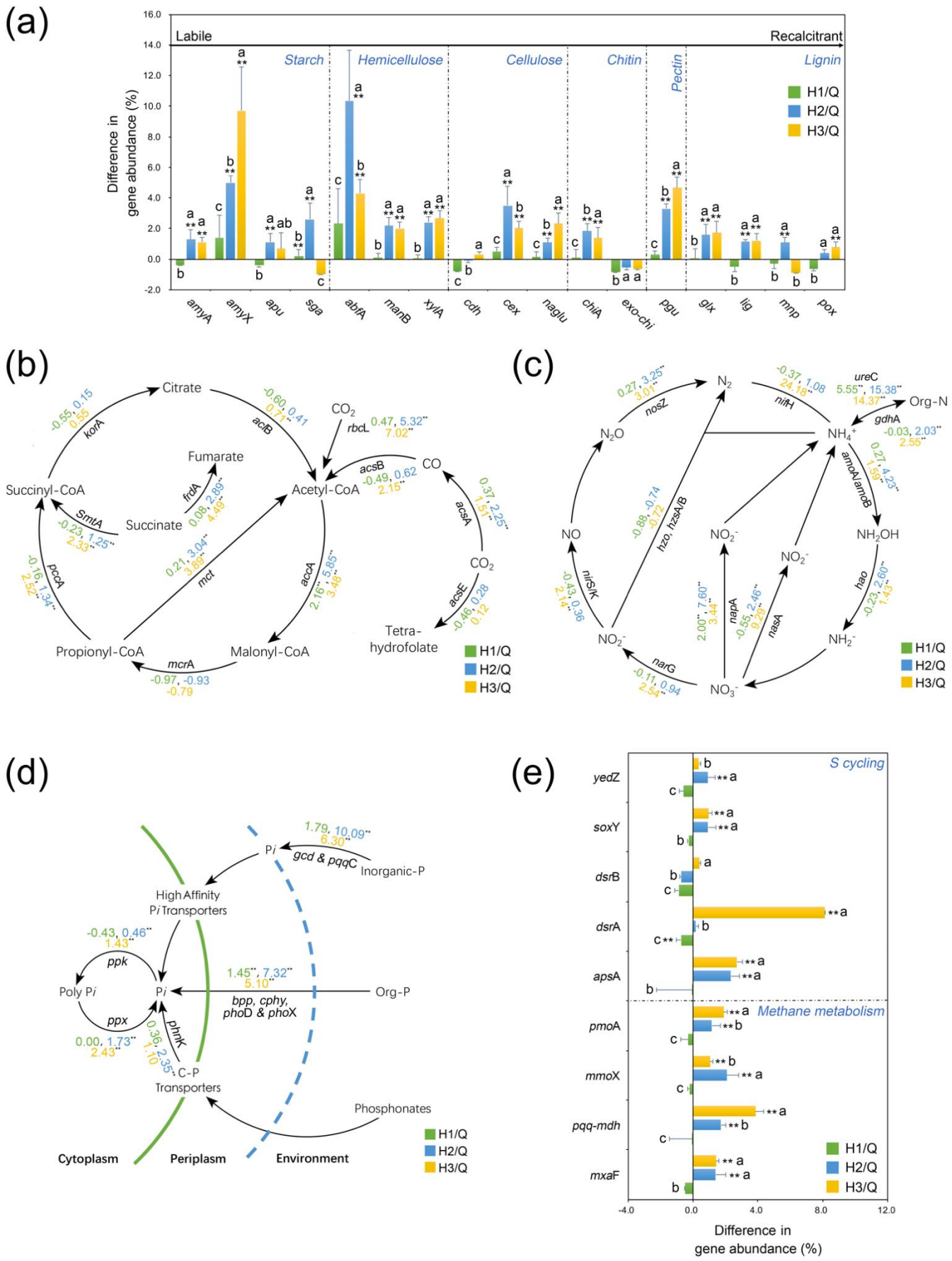

647

648 **Figure 3**